Int. J. Math. And Appl., 7(1)(2019), 121–136
ISSN: 2347-1557
Available Online: http://ijmaa.in/

International Journal of *Mathematics And its Applications*

MLS Method: Numerical Error and Solution of a Unilateral Contact Problem Using Penalty and Lagrange Multiplier

Rachid El Jid[1,*]

1 Department of Mathematics & Computing Sciences, Faculty of Sciences & Technology, University HASSAN I, Settat, Morocco.

Abstract: In this paper we propose a meshless approach (MLS) to solve two-dimensional unilateral contact problems. The convergence error of this method is studied, the element free Galerkin method and Galerkin formulation for two dimensional elasticity problems are considered. Then, the penalization method for the imposition of a contact constraint is proposed and the Lagrange multiplier method is used to impose essential boundary conditions. The implementation of the penalty / lagrange multiplier algorithm is described and the efficiency of our algorithm is illustrated by various examples.

MSC: 74G15, 74S30, 74B20, 74M15.

Keywords: Meshless Method, Moving Least Squares, Cnvergence error, Contact problem, Variational inequality, Penalty method, Lagrange multiplier method, Numerical experiment.

1. Introduction

The Contact problem appears within a large number of engineering problems such as extrusion, metal forming, machining and crash. This problem is one of the mostly used models in the theory of variational inequality [1]. Kikuchi and Oden [2], made a detailed analysis of the contact problem in elasticity with mathematical model and numerical implementation. Wang [3], improved the duality methods in the mixed finite element approximation. The phenomenon of contact in mechanical systems introduces dynamical boundary conditions that are normally inactive, but are enforced when parts of the moving mechanical structure come in contact. This introduces a greater level of complexity because it is not always known where or how contact occurs. Thus, unknown contact boundary and its change during the loading, and also the sliding of two bodies in frictional contact make the contact problem one of the most difficult nonlinear problems in the solid mechanics. Many studies have tried to bypass the difficulties of contact by using simulation methods. Most of the methods have used the finite element method to solve the problem [4–6]. Typically, two main constraint methods that have been employed in the finite element solution of contact problems are the method of Lagrange multipliers and the penalty approach. In Lagrange multipliers approach, the contact forces are taken as primary unknowns and the non-penetration condition is enforced [7, 8], these extra variables are added to the computational effort of the solution process. In the penalty method, the penetration between two contacting boundaries is introduced and the normal contact force is related to the penetration by a penalty parameter [4].

* *E-mail: rachideljid@gmail.com*

In recent years, meshless methods have been developed as alternative numerical approaches to eliminate known shortcomings of the mesh-based methods [9]. The main advantage of these methods is to approximate the unknowns by a linear combination of shape functions. Shape functions are based on a set of nodes and a certain weight function with a local support associated with each of these nodes. Therefore, they can solve many engineering problems that are not suited to conventional computational methods [10–12]. The moving least squares (MLS) [13] is an approximation method of constructing continuous functions from a set of unorganized sampled point values based on the calculation of a weighted least squares approximation. Since the numerical approximations starts from scattered nodes instead of interpolation on elements, there have been many meshless methods based on the MLS scheme for the numerical solution of differential equations. Typical of them are the element-free Galerkin method (EFGM) [14, 15], the HP meshless method [16], the MLS reproducing kernel method [18] and the meshless local Petrov Galerkin method [19, 20].

In this paper, the MLS method presented by Lancaster and Salkauskas [13] is discussed in details. The error estimation of the approximation function of the MLS method is presented. Then a hybrid penalty/Lagrange algorithm based on the MLS approach is proposed to solve the two dimensional unilateral contact problems. In this algorithm the penalization is used to impose the contact conditions and the Lagrange multiplier method is used to impose the essential boundary conditions. The efficiency of our algorithm is illustrated with various numerical examples.

2. Moving Least Squares Approximation

The MLS as an approximation method has been introduced by Shepard [13] and Lancaster and Salkauskas [14]. It consists of three components: a basis function, a weight function associated with each node, and a set of coefficients that depends on node position. Using MLS approximation, a data values $\mathbf{u} = \{u_i\}_{i=1}^{N}$ at nodes $\mathbf{x}_i$ is approximated by a function $u^h \in C^s\left(R^d\right)$ in a weighted square sense, namely.

$$u^h(\mathbf{x}) = \sum_{i=1}^{m} p_i(\mathbf{x})\, a_i(\mathbf{x}) = \mathbf{p}^T(\mathbf{x})\, \mathbf{a}(\mathbf{x}) \tag{1}$$

where $p_i(\mathbf{x})$, $i = 1, 2, \ldots, m$ are monomial basis functions, $\mathbf{p}^T(\mathbf{x}) = [p_1(\mathbf{x}), p_2(\mathbf{x}), \ldots, p_m(\mathbf{x})]$, m is the number of terms in the basis, and $a_i(\mathbf{x})$ are the coefficients of the basis functions. In general, the basis functions are as follows: For example, for a $1-$D problem, the linear basis is: $\{1, x\}$, and the quadratic basis is $\{1, x, x^2\}$. For a $2-$D problem, the linear basis is: $\{1, x, y\}$, and the quadratic basis is $\{1, x, y, x^2, xy, y^2\}$ where $\mathbf{x} = (x, y)$. The coefficient vector $\mathbf{a}(\mathbf{x})$ is determined by minimizing a weight discrete square norm, which is defined as

$$J(\mathbf{x}) = \sum_{i=1}^{N} w_i(\mathbf{x}) \left(\mathbf{p}^T(\mathbf{x})\, \mathbf{a}(\mathbf{x}) - u_i\right)^2 \tag{2}$$

where $w_i(\mathbf{x})$ is the weight function associated with the node i, N is the number of nodes in Ω for which the weight function $w_i(\mathbf{x}) > 0$ and u_i are the fictitious nodal values, but not the nodal values of the unknown trial function $u^h(\mathbf{x})$ i.e. $u^h(x_i) = u_i$. Equation (2) can be written as

$$J = [P.\mathbf{a}(\mathbf{x}) - \mathbf{u}]^T .W. [P.\mathbf{a}(\mathbf{x}) - \mathbf{u}],$$

where

$$P = \begin{bmatrix} p_1(\mathbf{x}_1) & p_2(\mathbf{x}_1) & \cdots & p_m(\mathbf{x}_1) \\ p_1(\mathbf{x}_2) & p_2(\mathbf{x}_2) & \cdots & p_m(\mathbf{x}_2) \\ \vdots & \vdots & \ddots & \vdots \\ p_1(\mathbf{x}_n) & p_2(\mathbf{x}_n) & \cdots & p_m(\mathbf{x}_n) \end{bmatrix} \quad and \quad W = \begin{bmatrix} w_1(\mathbf{x}) & 0 & \cdots & 0 \\ 0 & w_2(\mathbf{x}) & \cdots & 0 \\ \vdots & \vdots & \ddots & \vdots \\ 0 & 0 & \cdots & w_n(\mathbf{x}) \end{bmatrix}$$

The stationary point of J, in equation (2), with respect to $\mathbf{a}(\mathbf{x})$ leads to the following linear relation between $\mathbf{a}(\mathbf{x})$ and $\mathbf{u}$

$$A(\mathbf{x})\,\mathbf{a}(\mathbf{x}) = B(\mathbf{x})\,\mathbf{u}, \tag{3}$$

where the matrices $A(\mathbf{x})$ and $B(\mathbf{x})$ are defined by

$$A(\mathbf{x}) = P^T W P = B(\mathbf{x})\,P = \sum_{i=1}^{N} w_i(\mathbf{x})\,\mathbf{p}(\mathbf{x}_i)\mathbf{p}^T(\mathbf{x}_i), \tag{4}$$

$$B(\mathbf{x}) = P^T W = \left[w_1(\mathbf{x})\,\mathbf{p}(\mathbf{x}_1), w_2(\mathbf{x})\,\mathbf{p}(\mathbf{x}_2), \ldots, w_n(\mathbf{x})\,\mathbf{p}(\mathbf{x}_n)\right]. \tag{5}$$

The matrix A is often called the moment matrix, it is of size $m \times m$. Computing $a(x)$ using equation (3) and substituting it into equation (1), give

$$u^h(\mathbf{x}) = \Phi^T(\mathbf{x}).\mathbf{u} = \sum_{i=1}^{N} \Phi_i(\mathbf{x}).u_i, \quad \mathbf{x} \in \mathbf{\Omega} \tag{6}$$

where

$$\Phi^T(\mathbf{x}) = \mathbf{p}^T(\mathbf{x}) A^{-1}(\mathbf{x})\,B(\mathbf{x}), \tag{7}$$

and

$$\phi_i(\mathbf{x}) = \sum_{k=0}^{m} p_k(\mathbf{x}) \left[A^{-1}(\mathbf{x})\,B(\mathbf{x})\right]_{ki}. \tag{8}$$

$\phi_i(\mathbf{x})$ are called the shape functions of the MLS approximation, corresponding to nodal point $\mathbf{x}_i$. If $w_i(\mathbf{x}) \in C^r(\Omega)$ and $p_k(\mathbf{x}) \in C^s(\Omega)$, $i = 1, 2, \ldots, n$, $k = 0, 1, \ldots, m$, then $\phi_i(\mathbf{x}) \in C^{\min(r,s)}(\Omega)$. These form functions ϕ_i reproduce the basic functions

$$\sum_{i=1}^{N} \phi_i(x) x_i^p = x^p, 0 \le p \le m \tag{9}$$

and for $p_1(x) = 1$ we obtain the property of linear consistency also verified by the method of the finite elements

$$\sum_{i=1}^{N} \phi_i(x) = 1 \tag{10}$$

The usual choice for weight functions is a function that decreases with the distance with the node with which it is associated and which has the shape of a bell. If we pose $r = \frac{\|\mathbf{x}-\mathbf{x}_i\|}{d_i}$ where d_i is the support size of node $\mathbf{x}_i$., some common choices for wi (x) are:

- a truncated Gaussian:

$$w_i(\mathbf{x}) = \begin{cases} e^{-(\frac{r}{\alpha})^2}, & r \le 1 \\ 0, & r > 1 \end{cases} \tag{11}$$

which has the disadvantage of being discontinuous in $r = 1$ although this discontinuity goes unnoticed digitally if α is big enough;

- a modified Gaussian:

$$w_i(\mathbf{x}) = \begin{cases} \frac{e-(\frac{r}{\alpha})^2 - e-(\frac{1}{\alpha})^2}{1-e-(\frac{1}{\alpha})^2}, & r \le 1 \\ 0, & r > 1 \end{cases} \tag{12}$$

which is close to the previous one and is of class C^0;

- a cubic spline:

$$w_i(\mathbf{x}) = \begin{cases} \frac{2}{3} - 4r^2 + 4r^3, & r \le \frac{1}{2} \\ \frac{4}{3} - 4r + 4r^2 - \frac{4}{3}r^3, & \frac{1}{2} < r \le 1 \\ 0, & r > 1 \end{cases} \tag{13}$$

which is class C^1;

- a quartic spline :

$$w_i(\mathbf{x}) = \begin{cases} 1 - 6r^2 + 8r^3 - 3r^4, & r \leq 1 \\ 0, & r > 1 \end{cases} \tag{14}$$

which is class C^2. The experience shows that the results obtained vary little according to the chosen weight function. Subsequently, we will use this last spline of order 4. In two dimensions, circular and rectangular supports are usual.

Circular support:

$$w_i(x) = w_i\left(\frac{\|x_i - x\|}{d_i}\right)$$

Rectangular support:

$$w_i(x) = w_i\left(\frac{|x_i - x|}{d_i^x}\right) w_i\left(\frac{|y_i - y|}{d_i^y}\right)$$

Subsequently, we use a circular domain. The derivatives of the weight functions can be computed analytically. For example, for circular supports, we have

$$w_{i,k}(r) = w_i^{'}(r)\frac{x_k - x_{ik}}{rd_i^2} \tag{15}$$

In two dimensions and a square domain $[0.4] \times [0.4]$ with a regular distribution of 5×5 knots by choosing circular influence domain of support $d = 1.5$ one obtains the folowing figures that show the support (circlar support); the weight function and the function of form.

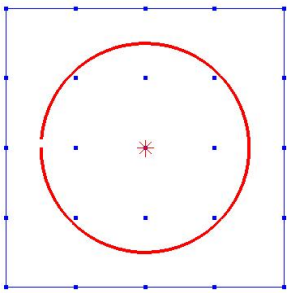

Figure 1: The support of the central node (red circle).

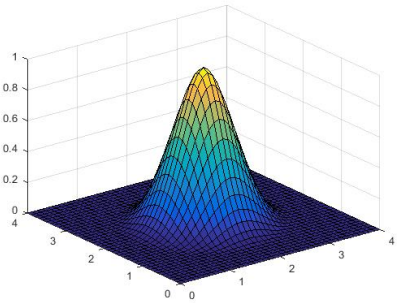

Figure 2: weight function at the central node

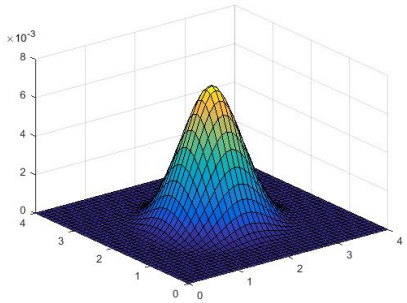

Figure 3: function of form at the central node

3. Convergence in the MLS Context

If we consider a space of functions for example, or other spaces, we know that different types of standard can be considered to measure different errors or quantities. In the context of MLS, we will also have a number of different standards depending on the context to be considered. Recall that the MLS approximation is written

$$u^{app}(x) = \sum_{x_i \in V(x)} u_i \phi_i(x) \tag{16}$$

where u_i means either numerically obtained nodal values $u^{num}(x_i)$, or the exact analytical values $u^{ex}(x_i)$ at the considered MLS node.

3.1. The numerical nodal error

L^∞-norm: The infinite nodal norm is defined by

$$\|U^{num} - U^{ex}\|_\infty = \sup_{1 \le i \le N} |u^{num}(x_i) - u^{ex}(x_i)| \tag{17}$$

where $u^{num}(x_i)$ denotes the value obtained numerically and $u^{ex}(x_i)$ denotes the analytical value. **L^2-norm:** The norm L^2 is defined by

$$\|U^{num} - U^{ex}\|_2 = \sum_{i=1}^{N} (u^{num}(x_i) - u^{ex}(x_i))^2 \tag{18}$$

3.2. Convergence in the case of a class solution C^{p+1}

The MLS u^{app} approximation can be compared to the exact solution $u^{ex}$the following theorems guarantee the convergence of the proposed method. Their proofs can be seen in [21].

Theorem 3.1.

$$\|u^{app} - u^{ex}\|_{L^\infty([0,L])} \le \frac{M}{(p+1)!} r^{p+1} \tag{19}$$

and

$$\|u^{app} - u^{ex}\|_{L^2([0,L])} \le \frac{M}{(p+1)!} r^{p+1} \tag{20}$$

Deriving $u^{ex} - u^{app}$, we obtain a remainder of order p in norm H^1.

$$\|u^{app} - u^{ex}\|_{H^1([0,L])} \le \frac{M}{p!} r^{p} \tag{21}$$

Theorem 3.2. *If we assume only $u^{ex} \in H^{p+1}$ and no more than class C^{p+1} then we get that*

$$\|u^{app} - u^{ex}\|_{L^2([0,L])} \le C r^{p+\frac{1}{2}} \|u^{ex}\|_{H^{p+1}([0,L])} \tag{22}$$

4. Discrete Equations for Elastostatics

Consider a domain Ω, bounded by Γ . The boundary is partitioned into two sets: Γ_u and Γ_t . Displacements $\overline{u}$ are prescribed on Γ_u whereas tractions $\bar{t}$ are prescribed on Γ_t. We define the spaces:

$$\begin{aligned} L_2(\Omega) &= \left\{ v : \textstyle\int_\Omega v^2 dx < \infty \right\}, \\ H^1(\Omega) &= \left\{ v \in L_2(\Omega) : \nabla v \in L_2(\Omega)^2 \right\}. \end{aligned}$$

and

$$H^1_{D,\overline{v}}(\Omega) = \left\{ v \in H^1(\Omega) : v = \overline{v}, \quad \text{on} \quad \Gamma_u \right\}.$$

In two dimensions the weak form of linear elastostatic problems consists to find $u \in H^1(\Omega)^2$ such that $u = \overline{u}$, on Γ_u and

$$\int_\Omega \varepsilon(u) : C : \varepsilon(v) d\Omega = \int_{\Gamma_t} \overline{t}.v d\Gamma + \int_\Omega f.v d\Omega, \quad \forall \ \ v \in H^1_{D,\overline{u}}(\Omega) \tag{23}$$

Substitution of approximations for u and v into the above gives the discrete equations:

$$Ku = F \tag{24}$$

with

$$K_{ij} = \int_\Omega B_i^T C B_j d\Omega \ \ and \ \ F_i = \int_{\Gamma_t} \Phi_i \overline{t} d\Gamma + \int_\Omega \Phi_i f d\Omega \tag{25}$$

In two dimensions, the B matrix is given by

$$B_i = \begin{pmatrix} \Phi_{i,x} & 0 \\ 0 & \Phi_{i,y} \\ \Phi_{i,y} & \Phi_{i,x} \end{pmatrix} \tag{26}$$

In the meshless method, we use the shape functions obtained by the MLS approximation and the equations that describe the finite element method are still valid to describe this method. The choice of shape functions leads to two different points; one in the imposition of boundary conditions and the other for the numerical integration.

4.1. Essential Boundary Conditions

In lack of the Kronecker delta property of MLS shape functions, the essential boundary conditions cannot be imposed as easily as in finite element method. Several techniques have been proposed, namely the methods based on the modification of the weak form and the methods using modified shape functions. The methods based on the modification of the weak form, we use in this work, include the Lagrange multiplier method and the penalty method. To understand these methods we first introduce the variational principle. A variational principle specifies a scalar quantity, named functional Π, defined by:

$$\Pi(u) = \int_\Omega F(u, u_x, ...) d\Omega + \int_\Gamma E(u, u_x, ...) d\Gamma \tag{27}$$

where u is the unknown function, F and E are differential operators.

Lagrange Multiplier Method

We consider a general problem of a Π functional stationary with constraints:

$$C(u) = 0 \ \ on \ \ \Gamma \tag{28}$$

To satisfy the above constraint, we build the following functional:

$$\overline{\Pi}(u, \lambda) = \Pi(u) + \int_\Gamma \lambda^T C(u) d\Gamma \tag{29}$$

The variation of this new functional is given by

$$\delta\overline{\Pi}(u, \lambda) = \delta\Pi(u) + \int_\Gamma \delta\lambda^T C(u) d\Gamma + \int_\Gamma \lambda^T \delta C(u) d\Gamma \tag{30}$$

In order to derive the discrete equations, the Lagrange multipliers must be approximated (if l is the number of shape functions required to approximate the multipliers on the boundary:

$$\lambda(x) = \sum_{i=1}^{l} N_i(x)\lambda_i \tag{31}$$

There are several choices for the approximation space for the Lagrange multipliers, i.e. choices of $N_i(x)$, namely, finite element interpolation on the boundary Γ or meshless approximations on this boundary. Using the first method, the system of equations of elastostatics is given by

$$\begin{bmatrix} K & G \\ G^T & 0 \end{bmatrix} \begin{bmatrix} u \\ \lambda \end{bmatrix} = \begin{bmatrix} F \\ q \end{bmatrix} \tag{32}$$

with

$$G_{ij} = -\int_{\Gamma_u} \Phi_i N_j d\Gamma \tag{33}$$

$$q_j = -\int_{\Gamma_u} N_j \overline{u} d\Gamma \tag{34}$$

It is obvious that one drawback of the Lagrange multipliers method is the introduction of additional unknowns to the problem.

Penalty method

for the penalty method we have the following functional:

$$\overline{\Pi}(u, \alpha) = \Pi(u) + \frac{\alpha}{2} \int_{\Gamma} C(u)^T C(u) d\Gamma \tag{35}$$

Applying the penalty method to elastostatics, we obtain the following weak form:

$$\int_{\Omega} \varepsilon^T(u) : C : \varepsilon(v) d\Omega = \int_{\Gamma_t} \overline{t}.v d\Gamma + \int_{\Omega} f v d\Omega + \alpha \int_{\Gamma_u} uv d\Gamma - \alpha \int_{\Gamma_u} \overline{u} v d\Gamma \tag{36}$$

which gives the equation Ku = F, where

$$K_{ij} = \int_{\Omega} B_i^T C B_j d\Omega - \alpha \int_{\Gamma_u} \Phi_i \Phi_j d\Gamma \tag{37}$$

$$F_i = \int_{\Gamma_t} \Phi_i \overline{t} d\Gamma + \int_{\Omega} \Phi_i f d\Omega - \alpha \int_{\Gamma_u} \Phi_i \overline{u} d\Gamma \tag{38}$$

The main advantage of the penalty method compared with the Lagrange multiplier approach is that no additional unknowns are required. However, the conditioning of the matrix much depends on the choice of the penalty parameter. What is more, in the penalty method, the constraints are only satisfied approximately. In this paper, the penalization method is used for the imposition of a contact constraint and the Lagrange multipliers method is used to impose essential boundary conditions.

4.2. Numerical integration

The major disadvantage of meshless methods using Galerkin method is the numerical integration of the weak form. This is due to the non-polynomial (rational) form of most meshless shape functions (MLS for instance). So, exact integration is difficult to impossible for most meshfree methods. The most used numerical techniques are presented bellow.

Direct nodal integration

The integrals are evaluated only at the nodes that also serve as integration points:

$$\int_{\Omega} f(X)d\Omega = \sum f(X_j)V_j \tag{39}$$

The quadrature weights V_j are usually volume associated with the nodes. The volume is obtained from a Voronoi diagram constructed at the beginning of the computation. This approach is more efficient than using full integration. However, nodal integration leads to instabilities due to rank deficiency similar to reduced integrated finite elements.

Stabilized nodal integration

The stabilized confirming nodal integration using strain smoothing is presented in [22] and detailed in [23]. the authors recognized that the vanishing derivatives of the meshfree shape functions at the particles cause of the instabilities. In their strain smoothing procedure, the nodal strains are computed as the divergence of a spatial average of the strain field. The strain smoothing avoids evaluating derivatives of the shape functions at the nodes and hence eliminates defective nodes.

Support-based integration

In the method of finite spheres, the integration is performed on every intersections of overlapping supports. Duflot and Nguyen-Dang [24] and Carpinteri [25] have developed a meshfree method for integrating the weak form over overlapping supports, related to the supports of the meshfree approximation. This integration technique is improved in Carpinteri [26] and Zhang [27] to take cracks into account.

Background mesh or cell structure

In this method, the domain is divided into integration cells over which Gaussian quadrature is performed:

$$\int_{\Omega} f(X)d\Omega = \sum_{j} f(\xi_j)\omega_j detJ^{\xi}(\xi) \tag{40}$$

where ξ are local coordinates and $detJ^{\xi}(\xi)$ is the determinant of the Jacobian, i.e. the mapping from the parent into the physical domain. If a background mesh is present, nodes and the vertices of the integration usually coincide (as in conventional FEM meshes). When cell structures are utilized, a regular array of domains is created independently of the particle position [27]. In this paper we will consider only methods that employ Gauss quadrature and utilize a background mesh. These methods are more accurate and they are ideally applicable to small and moderate deformation.

5. The Implementation of a 2D Unilateral Contact Problems by Penalty/MLS

5.1. Problem formulation

We consider two elastic bodies Ω_1 and Ω_2 (Figure 1). We denote $\Omega = \Omega_1 \bigcup \Omega_2$, and n_i is the unit normal outward to the domain boundary Γ_i of Ω_i.

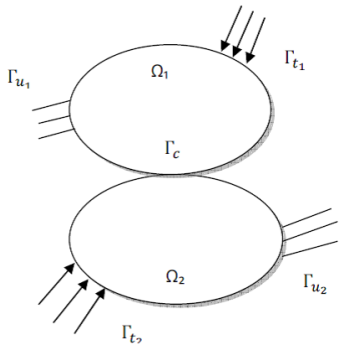

Figure 4: Elastic bodies in contact.

The classical equations of elasticity problem are

$$\begin{cases} div\sigma + f = 0 & \text{in } \Omega \\ \sigma = C\varepsilon & \text{in } \Omega \\ \sigma n = \overline{t} & \text{on } \Gamma_t \\ u = \overline{u} & \text{on } \Gamma_u \end{cases} \tag{41}$$

where $\overline{u}$ is the prescribed displacement on the essential boundary, $\Gamma_u = \Gamma_{u_1} \cup \Gamma_{u_2}$ and $\overline{t}$ the prescribed traction on the natural boundary, $\Gamma_t = \Gamma_{t_1} \cup \Gamma_{t_2}$. The contact interface consists of the intersection of the surfaces of the two bodies, and is shown by Γ_c with $\Gamma_c = \Gamma_{c_1} \cap \Gamma_{c_2}$. In Γ_c we set $n = n_1 = -n_2$. We decompose the displacement u into u_1 and u_2 onto Ω_1 and Ω_2 respectively and it is the same for the stress tensor σ and the strain ε.

The normal force is denoted by:

$$\overline{t}_{i_n} = n_i \sigma_i n_i, \quad i = 1, 2 \tag{42}$$

and the tangential force is denoted by:

$$\overline{t}_{i_t} = \sigma_i n_i - \overline{t}_{i_n} n_i, \quad i = 1, 2 \tag{43}$$

The contact conditions on Γ_c are:

$$(u_2 - u_1)n \geq 0 \tag{44}$$

$$\overline{t}_n = \overline{t}_{1_n} = -\overline{t}_{2_n} \leq 0 \tag{45}$$

$$\overline{t}_t = \overline{t}_{1_t} = -\overline{t}_{2_t} = 0 \tag{46}$$

$$(u_2 - u_1).n\overline{t}_n = 0 \tag{47}$$

Under these conditions the classical formulation of our problem is as follows:

$$\begin{cases} div\sigma + f = 0 & \text{in } \Omega \\ \sigma = C\varepsilon & \text{in } \Omega \\ \sigma n = \overline{t} & \text{on } \Gamma_t \\ u = \overline{u} & \text{on } \Gamma_u \\ (u_2 - u_1)n \geq 0 & \text{on } \Gamma_c \\ (u_2 - u_1)n\overline{t}_n = 0 & \text{on } \Gamma_c \\ \overline{t}_n = \overline{t}_{1_n} = -\overline{t}_{2_n} \leq 0 & \text{on } \Gamma_c \\ \overline{t}_t = \overline{t}_{1_t} = -\overline{t}_{2_t} & \text{on } \Gamma_c \end{cases} \tag{48}$$

5.2. Weak formulation

We introduce the spaces

$$U_{ad} = \{v \in H^1(\Omega) \ / \ v = \overline{u} \ on \ \Gamma_u\} \ \ and \ \ K = \{v \in U_{ad} \ / \ \ (v_2 - v_1)n \geq 0 \ on \ \Gamma_c\}$$

The weak formulation of the problem (48) is as follows:

Find a displacement field $u \in K$ such as, for all $v \in K$, we have

$$\int_{\Omega_1} \sigma_1 : \varepsilon(v_1 - u_1)d\Omega + \int_{\Omega_2} \sigma_2 : \varepsilon(v_2 - u_2)d\Omega = \int_{\Omega_1} f(v_1 - u_1)d\Omega + \int_{\Omega_2} f(v_2 - u_2)d\Omega + \int_{\Gamma_{t_1}} \overline{t}_1(v_1 - u_1)d\Gamma \tag{49}$$

$$+ \int_{\Gamma_{t_2}} \overline{t}_2(v_2 - u_2)d\Gamma + \int_{\Gamma_{c_1}} \sigma_1 n_1(v_1 - u_1)d\Gamma + \int_{\Gamma_{c_2}} \sigma_2 n_2(v_2 - u_2)d\Gamma. \tag{50}$$

then

$$\int_{\Omega} \sigma : \varepsilon(v - u)d\Omega = \int_{\Omega} f(v - u)d\Omega + \int_{\Gamma_t} \overline{t}(v - u)d\Gamma + \int_{\Gamma_{c_1}} \sigma_1 n_1(v_1 - u_1)d\Gamma + \int_{\Gamma_{c_2}} \sigma_2 n_2(v_2 - u_2)d\Gamma. \tag{51}$$

We define

$$a(u, v - u) = \int_{\Omega} \sigma : \varepsilon(v - u)d\Omega \quad \ and \ \ l(v - u) = \int_{\Omega} f(v - u)d\Omega + \int_{\Gamma_t} \overline{t}(v - u)d\Gamma. \tag{52}$$

then, we obtain

$$a(u, v - u) - l(v - u) = \int_{\Gamma_{c_1}} \sigma_1 n_1(v_1 - u_1)d\Gamma + \int_{\Gamma_{c_2}} \sigma_2 n_2(v_2 - u_2)d\Gamma \tag{53}$$

Using equations (45) and(46) we get:

$$a(u, v - u) - l(v - u) = \int_{\Gamma_{c_1}} \overline{t}_n(v_1 - u_1)nd\Gamma - \int_{\Gamma_{c_2}} \overline{t}_n(v_2 - u_2)nd\Gamma. \tag{54}$$

or

$$a(u, v - u) - l(v - u) = \int_{\Gamma_{c_1}} \overline{t}_n(u_2 - u_1)nd\Gamma - \int_{\Gamma_{c_2}} \overline{t}_n(v_2 - v_1)nd\Gamma. \tag{55}$$

By equations (45) and (47), we have

$$\int_{\Gamma_c} \overline{t}_n(v_2 - v_1)nd\Gamma \leq 0 \quad and \ \int_{\Gamma_{c_1}} \overline{t}_n(u_2 - u_1)nd\Gamma = 0 \tag{56}$$

The weak formulation becomes: Find a displacement field $u \in K$ such as for all $v \in K$ we have

$$a(u, v - u) - l(v - u) \geq 0 \tag{57}$$

The nonlinearity due to the unilateral constraints makes it difficult to solve the contact problem directly. For this reason, an equivalent minimization problem is formulated which is particularly suitable for numerical implementation. It can be shown [1] that the optimization problem: Find $u \in K$ which minimizes the potential energy

$$E_c(v) = \frac{1}{2}a(v, v) - l(v). \tag{58}$$

is equivalent to the contact problem (57).

In this paper we propose a numerical resolution strategies using the penalty method.

5.3. The implementation of the penalty method

The penalty methods avoid the need for additional variables by introducing an approximation of the constraint conditions. An additional term enters in the weak form of the governing equations, which penalizes the dissatisfaction of the constraint conditions by a positive penalty parameter. Physically, this regulation is interpreted as follows: we accept that in the contact zone there is a slight penetration; the condition (44) is abandoned and we assume that $g = (u_2 - u_1)n$ can take negative values and sufficiently small by relative to the dimensions of solids (see Fig5). The penalty term is introduced as follows:

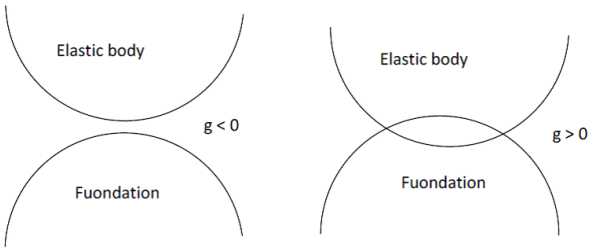

Figure 5: Bodies before and after interpenetrating.

$$\bar{E_c}(u) = E_c(u) + \frac{\alpha}{2} g^t g \tag{59}$$

According to the minimum potential energy principle, the first variation of the total potential energy is equal to zero. Therefore, the following linear system is obtained:

$$\delta E_c(u) + \alpha g^t \delta g = 0 \tag{60}$$

By enforcing the essential boundary using Lagrange multiplier as in (30), the potential energy in the entire solution domain can be given by:

$$\int_\Omega \sigma(u) : \varepsilon(v) d\Omega - \int_\Omega f.v d\Omega - \int_{\Gamma_t} \overline{t}.v d\Gamma - \int_{\Gamma_u} \delta\lambda.(u - \overline{u}) d\Gamma - \int_{\Gamma_u} v.\lambda d\Gamma + \alpha \int_{\Gamma_C} g\delta g H(g) d\Gamma = 0 \tag{61}$$

where α is the penalty parameter and H is the Heaviside step defined by:

$$H(g) = \begin{cases} 1 \quad if \quad g \leq 0 \\ 0 \quad if \quad g > 0 \end{cases} \tag{62}$$

To discretize the contact interface, the interpenetration g can be discretized as follows:

$$g = \phi u \quad et \quad \delta g = \phi \delta u \tag{63}$$

We have

$$\alpha \int_{\Gamma_C} g\delta g H(g) d\Gamma = \alpha \int_{\Gamma_C} \phi^T \delta u \phi u H(u) d\Gamma = P_c \delta u, \quad \forall \delta u \tag{64}$$

with

$$P_c = \alpha \int_{\Gamma_C} \phi^T \phi H(u) d\Gamma u = K_c u \tag{65}$$

where K_c is the contact matrix for small-displacement elastostatic and defined as:

$$K_c = \alpha \int_{\Gamma_C} \phi^T \phi H(u) d\Gamma. \tag{66}$$

Using (66) and (61) we obtain the system:

$$\begin{bmatrix} K_T & G \\ G^T & 0 \end{bmatrix} \begin{bmatrix} u \\ \lambda \end{bmatrix} = \begin{bmatrix} F \\ q \end{bmatrix}, \tag{67}$$

where

$$K_T = K + K_c$$

To implement the contact in our mshelss code, the following algorithm is considered:

- For a well chosen α (penalty parameter) and TOL (tolerance), we have
- Compute K , G, F and q
- iter $= 0$ and a given u_0
- **while** iter > 0
  - **begin**
  - Find contact nodes of the bodie
  - Compute K_c
  - Solve (67)
  - if $\frac{\|U_{k+1}-U_k\|}{\|U_k\|} < TOL$
  - **end**
  - else
  - iter=iter+1
- **end**

6. Numerical Examples

Example 6.1. *In this first example we consider a rectangular plate of dimension $L \times D$ which is in frictionless contact with a rigid foundation (Figure 6), where $L = 40mm$, $D = 10mm$.*

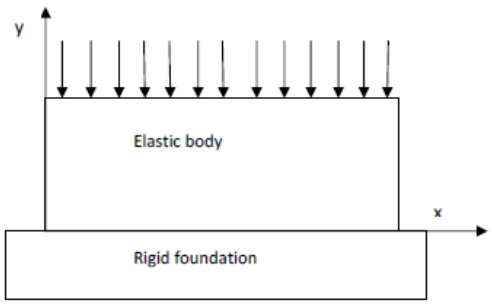

Figure 6: Elastic body in contact with a rigid foundation.

The material behavior will be isotropic linear elastic with $E = 3.10^4 MPa$, $\upsilon = 0.3$ and a load $P = 10MPa$. The considered boundary conditions are $u_x(0, .) = 0$ and $u_x(L, .) = 0.$. For a nodal distribution 25x15 nodes we obtain the following results:

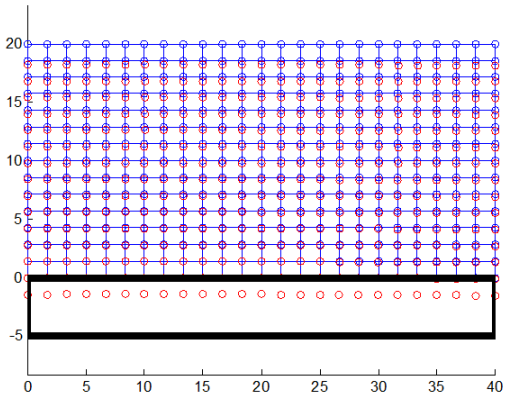

Figure 7: Deformation of the structure for $\alpha = 10^2$, the deformation is in red color.

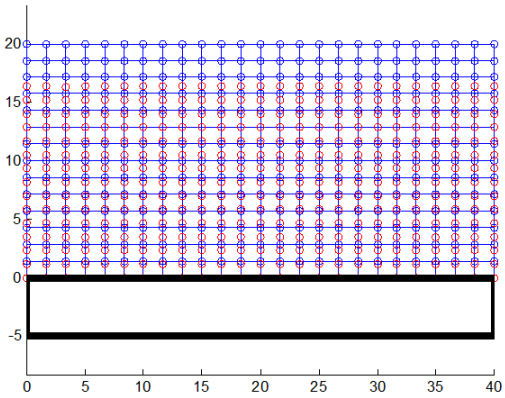

Figure 8: Deformation of the structure for $\alpha = 10^9$, the deformation is in red color.

In Figure 7, where $\alpha = 10^2$, we see that there is interpenetration between the two bodies. however, when $\alpha = 10^9$ there is no interpenetration (Figure 8). To study the effect of the contact penalty parameter, the vertical displacement is shown in (Figure 9).

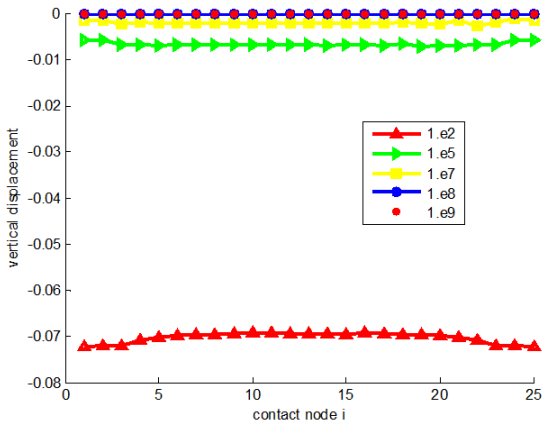

Figure 9: Vertical displacement for different values of contact penalty parameter.

We note that the more the penalty parameter increases, the more the vertical displacement of the contact nodes decreases, and it is observed that by choosing the penalty parameter of the order of $\alpha = 10^8$, the interpenetration is almost zero and the conditions of Signorini are met.

Example 6.2. *In this second example we consider a rectangular plate of dimension $L \times D$ fixed at both ends, where $L = 60mm$, $D = 30mm$. The plate is in frictionless contact with a rigid foundation and the material behavior will be isotropic linear elastic with $E = 21.10^3 MPa$, $\upsilon = 0.3$ and a load $P = 10MPa$. The boundary conditions are $u_x(0,.) = u_y(0,.) = 0$ and $u_x(L,.) = u_y(L,.) = 0$.*

For a nodal distribution 30×15 nodes we obtain the following results:

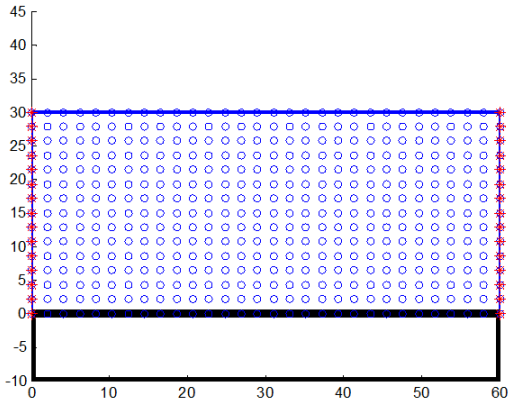

Figure 10: Distribution of nodal 30×15 nodes.

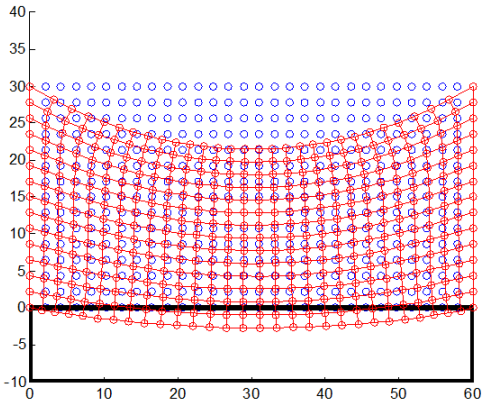

Figure 11: Deformation of the structure for $\alpha = 10^2$, the deformation is in red color.

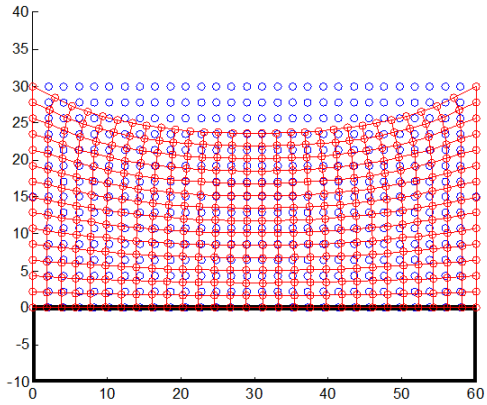

Figure 12: Deformation of the structure for $\alpha = 10^8$, the deformation is in red color.

To study the effect of the contact penalty parameter, the vertical displacement is shown in (Figure 13).

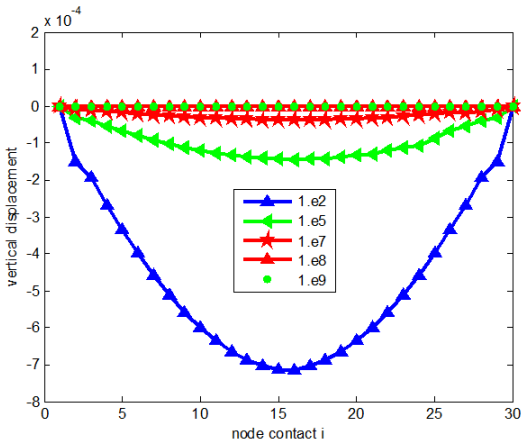

Figure 13: Vertical displacement for different values of contact penalty parameter.

In this second example, the study confirms the effect of the penalty parameter that has been proved in the previous example. In addition, the value of this parameter which leads to the respect of the Signorini conditions is always of the order of $\alpha = 10^8$.

7. Conclusion

In this paper the MLS methd is described in detail, its convergence error is studied. A penalty / Lagrange algorithm based on the MLS approach is proposed to solve the two dimensional unilateral contact problems.The penalty method was used for the imposition of the contact constraint and the Lagrange multiplier method was employed to impose essential boundary conditions. The method was evaluated by using several tests. The results showed a good performance of the proposed method. Also, the final formulation of the method proves its simplicity and feasibility. The future development is promising for more complex problems.

References

[1] G. Duvaut and J. L. Lions, *Les ingalites variationnelles en mcanique et en physique*, Dunod, Paris, (1972).

[2] N. Kikuchi and J. T. Oden, *Contact problems in Elasticity*, SIAM Philadelphia, (1988).

[3] L. Wang, *On the duality methods for the contact problem in elasticity*, Comput. Methods Appl. Mech. Engrg., 167(1998), 275-282.

[4] D. Peric and J. Owen, *Computational model for 3D contact problems with friction based on the penalty method*, Int. J. Num. Meth. Eng., 35(1992), 1289-1309.

[5] P. Wriggers, *Computational contact mechanics*, 2nd Ed., Springer, (2006).

[6] P. Hild and P. Laborde, *Quadratic finite element methods for unilateral contact problems*, Appl. Numer. Math., 41(2002), 401-421.

[7] W. Ju and R. L. Taylor, *A perturbed Lagrange formulation for the finite element solution of nonlinear frictional contact problems*, J. Theo. App. Mech.,7(1988), 1-14.

[8] J. C. Simo and T. A. Laursen, *An augmented Lagrangian treatment of contact problems involving friction*, Comp. and Struc., 42(1992), 97-116.

[9] T. Belytschko, Y. Krongauz and D. Organ, *Meshless methods: an overview and recent developments*, Comput. Methods Appl. Mech. Eng., 139(1996), 3-47.

[10] Y. Cheng, J. Wang and R. Li, *The complex variable element-free Galerkin method for two-dimensional elastodynamics problems*, Int. J. Appl. Mech., 4(2012).

[11] H. Ren and Y. Cheng, *The interpolating element-free Galerkin (IEFG) method for two-dimensional potential problems*, Eng. Anal. Boundary Elem., 36(2012), 873-880.

[12] B. Zheng and B. Dai, *A meshless local moving Kriging method for two-dimensional solids*, Appl. Math. Comput., 218(2011), 563-573.

[13] D. Shepard, *A two-dimensional interpolation function for irregularly spaced points*, Proc. 23rd Nat. Conf. ACM, ACM Press, New York, (1968), 517-524.

[14] P. Lancaster and K. Salkauskas, *Surface generated by moving least squares methods*, Math. Comput., 37(1981), 141-158.

[15] T. Belytschko, Y. Krongauz, D. Organ, M. Fleming and P. Krysl, *Meshless methods: An overview and recent developments*, Comput. Methods Appl. Mech. Engrg., 139(1996), 3-47.

[16] L. Zhang, J. Ouyang and X. Zhang, *On a two-level element-free Galerkin method for incompressible fluid flow*, Appl. Numer. Math., 59(2009), 1894-1904.

[17] C. A. Duarte and J. T. Oden, *Hp clouds An hp meshless method*, Numer. Methods Part. Differ. Equat., 12(1996), 675-705.

[18] W. K. Liu, S. Li and T. Belytschko, *Moving least-square reproducing kernel methods: methodology and convergence*, Comput. Methods Appl. Mech. Engrg., 143(1997), 113-154.

[19] S. N. Atluri and S. P. Shen, *The meshless local Petrov Galerkin (MLPG) method: A simple less-costly alternative to the finite element and boundary element methods*, CMES: Comput. Modeling Eng. Sci., 3(2002), 11-51.

[20] M. Dehghan and D. Mirzaei, *Meshless Local Petrov Galerkin (MLPG) method for the unsteady magnetohydro dynamic (MHD) flow through pipe with arbitrary wall conductivity*, Appl. Numer. Math., 59(2009), 1043-1058.

[21] R. EL JID, *Moving least squares and gauss legendre for solving the integral equations of the second kind*, IAENG International Journal of Applied Mathematics, 49(1)(2019), 90-97.

[22] J. S. Chen, C. T. Wu, S. Yoon and Y. You, *A stabilized conforming nodal integration for Galerkin meshfree-methods*, Int. J. Numer. Methods Eng., 50(2001), 435-466.

[23] M. A. Puso, J. S. Chen, E. Zywicz and W. Elmer, *Meshfree and finite element nodal integration methods*, Int. J. Numer. Methods Eng., 74(2008), 416-446.

[24] M. Duflot and H. Nguyen-Dang, *A truly meshless method based on a moving least squares quadrature*, Commun. Numer. Methods Eng., 18(2002), 441-449.

[25] A. Carpinteri, G. Ferro and G. Ventura, *The partition of unity quadrature in meshless methods*, Int. J. Numer. Methods Eng., 54(2002), 987-1006.

[26] A. Carpinteri, G. Ferro and G. Ventura, *The partition of unity quadrature in element-free crack modelling*, Comput. Struct., 81(2003), 1783-1794.

[27] Z. Q. Zhang, J. X. Zhou, X. M. Wang, Y. F. Zhang and L. Zhang, *Investigations on reproducing kernel particle method enriched by partition of unity and visibility criterion*, Comput. Mech., (2004).

[28] J. Dolbow and T. Belytschko, *Numerical integration of the Galerkin weak form in meshfree methods*, Comput. Mech., 23(1999), 219-230.